Organometallic precursors to the formation of GaN by MOCVD: structural characterisation of Me₃Ga · NH₃ by gas-phase electron diffraction

Matthew J. Almond, Carolyn E. Jenkins, David A. Rice

Department of Chemistry, University of Reading, Whiteknights, P.O. Box 224, Reading RG6 2AD (UK)

and Kolbjørn Hagen

Department of Chemistry, University of Trondheim, N7055 Trondheim (Norway)

(Received April 3, 1992)

Abstract

The molecular structure of $Me_3Ga \cdot NH_3$ [I] has been studied by gas-phase electron diffraction at 25°C. The experimental data are fitted by a model in which the C_3–Ga–N core of the molecule has C_{3v} symmetry. The molecule was defined in terms of four bond distances, three valence angles and two torsion angles. Of the bond distances three were refined (r_g(Ga–N) = 2.161(22) Å, r_g(Ga–C) = 1.979(3) Å, r_g(C–H) = 1.109(7) Å). It was necessary to hold the fourth bond distance at an assumed value [r_g(N–H) = 1.045 Å]. Two of the valence angles were refined (N–Ga–C = 101.8(62)°, Ga–C–H = 111.3(16)°) with the third (Ga–N–H) being held at 109.0°. The torsion angle H–N/Ga–C was held at 60.0° while the remaining torsion angle H–C/Ga–N was refined to 37.5(224)°. The dependent angle C–Ga–C was 115.9(42)°, so the C_3Ga fragment is not far from planar, which is in accord with the lone pair from the nitrogen atom being donated into the p_z orbital on the gallium atom. This suggestion is supported by the gas-phase and low temperature infra-red spectroscopic data that are reported. Evidence is also presented suggesting the Ga–N bond is weak and thus it is not surprising that when NH_3 and Me_3Ga are used to grow GaN it is necessary to use NH_3/Me_3Ga ratios greater than one.

Introduction

Binary compounds of elements from Groups IIIB and VB – the so-called III–V compounds – are attracting increased attention as they have properties that make them useful as electronic and optoelectronic materials [1]. Metal Organic Chemical Vapour Deposition (MOCVD) is one process employed to manufacture thin, epitaxial layers of the III–V compounds. Gaseous precursors are passed over a

---

Correspondence to: Dr. D.A. Rice.

heated substrate upon which they decompose to give the desired compound. Common precursors to GaN are Me_3Ga and NH_3 [2]. The reactions that take place between Me_3Ga and NH_3 are only partially understood, but it is believed that the Lewis acid–Lewis base adduct, $Me_3Ga \cdot NH_3$, [I], is formed initially. This white crystalline adduct may be made at room temperature by coordination of NH_3 to Me_3Ga [3]. Although the adduct has been isolated, it has not been adequately characterised and more information is desirable. A clearer picture of the nature of the bonding within such species might help in achieving an understanding of the reaction pathways that lead to GaN formation.

The isolation of I was first reported by Kraus and Toonder in 1933 [4]. The infrared and Raman spectra of the adduct in the solid state at 77 K have been recorded [5]. However, little is known of its gas-phase structure. Indeed, to this date, $Me_3Ga \cdot NMe_3$ is the only amine adduct of Me_3Ga whose structural characterisation by gas electron diffraction has been reported [6].

The aim of this present study was to use gas-phase electron diffraction to characterise the adduct I structurally. In the context of the use of I in the MOCVD technique the determination by electron diffraction of the gas-phase structure [as opposed to that in the solid state] is of particular importance as in both MOCVD and gas-phase electron diffraction a flow of gaseous material is used.

Experimental

The samples were prepared and transferred in an all-glass high vacuum system fitted with Young's greaseless taps. Trimethylgallium was kindly supplied by Professor D.J. Cole-Hamilton and was purified by vacuum distillation before use. Ammonia gas (BOC) was dried over sodium and degassed before use. The adduct I was prepared by the condensation with Me_3Ga of a slight molar excess of NH_3. The mixture was allowed to stand at room temperature and the excess of NH_3 removed by distillation.

Infra-red spectra (solid phase) were recorded between 4000 and 180 cm^{-1} on a Perkin-Elmer model 983 dispersive spectrophotometer. The samples were deposited slowly, under a dynamic vacuum, onto a CsI window in contact with a reservoir of liquid nitrogen, *via* a brass holder supported on an evacuated glass shroud. Spectral data were measured with an accuracy of ± 2 cm^{-1}. The spectrum of the gaseous adduct in a 10 cm path-length cell fitted with CsI windows was recorded on a Perkin-Elmer 1720X Fourier transform instrument.

The purity of the sample was assessed by mass spectrometric and ^1H NMR spectroscopic analysis. A sample for NMR spectroscopy was prepared, in an oxygen-free nitrogen-filled dry box, by loading the solid into an NMR tube (fitted with a cone and socket). A small amount of Na-dried benzene-d_6 (Aldrich) was used to dissolve the sample. The tube was subsequently sealed to exclude air and moisture. The spectrum was recorded on a Jeol FX 90Q Fourier transform spectrometer. The chemical shifts were measured relative to benzene (7.13 ppm). The ^1H NMR spectrum of I in C_6D_6 solution showed a signal corresponding to the methyl protons on the gallium atoms at -0.22 ppm (singlet) but no signal due to the N–H protons was observed because of the effect of nuclear quadrupole broadening. No evidence for NH_3 or Me_3Ga impurities was found in the infra-red spectrum of either (a) the solid at 77 K or (b) the vapour.

The 70 eV mass spectrum of the vapour above a sample of the adduct was recorded using a Vacuum Generator SXP800 Spectramass quadrupole spectrometer, controlled by a Spectralab version 4 computer program.

Gas-phase electron diffraction

Gas-phase electron diffraction data of the adduct I were obtained at the University of Oslo from the Balzers Eldigraph KDG-2 apparatus [7]. The nozzle-to-plate distances were 496.73 and 246.81 mm and the data were obtained with the nozzle at 25°C. The electron wavelength [0.058690 Å] was calibrated against diffraction patterns of benzene [8].

Six plates from each camera distance were traced on the microdensitometer for the final analysis. The data, covering the ranges $2.00 \leqslant s \leqslant 15.00$ Å^{-1} and $4.00 \leqslant s \leqslant 30.00$ Å^{-1} at intervals of $\Delta s = 0.25$ Å^{-1}, were processed as previously described [9] with published scattering factors [10]. The average curves produced for each camera distance are shown in Fig. 1 together with the theoretical curve and the difference curves.
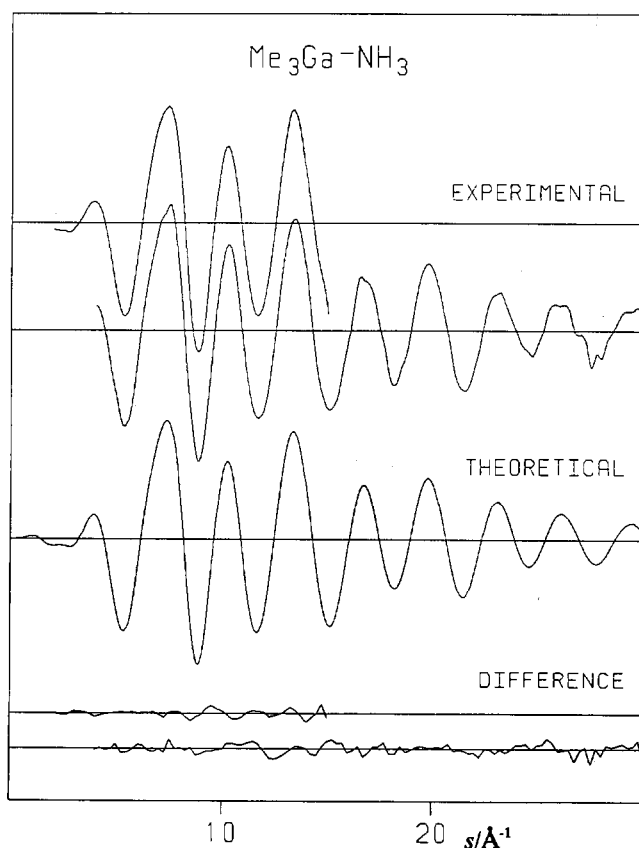

Fig. 1. Experimental, theoretical and difference intensity curves for Me$_3$Ga·NH$_3$.

Analysis of the structure of Me₃Ga · NH₃

The refinements of the structure were based upon the molecular model illustrated in Fig. 2, in which is given the atom numbering scheme. It was assumed that

1) the C_3GaN fragment has C_{3v} symmetry;

2) all methyl groups are identical and have local C_{3v} symmetry with the axis of symmetry being along the Ga–C bond and all C–H bonds of the same length;

3) all N–H bonds are of the same length and the NH_3 moiety has C_{3v} symmetry about the Ga–N bond.

With the above constraints a model based upon nine parameters was constructed. These consisted of the distances r(Ga–N), r(N–H), r(Ga–C), r(C–H), the angles Ga–N–H, N–Ga–C, Ga–C–H and two torsion angles. The first torsion angle, ϕ_1, defines the position of the H–C bonds with respect to the Ga–N bond *i.e.* $\phi_1 = \tau_1$(HCGaN) (rotation about Ga–C). The other torsion angle, ϕ_2, describes the position of the H–N bonds with respect to the Ga–C bonds *i.e* $\phi_2 = \tau_2$(HNGaC) (rotation about Ga–N).

Root mean square amplitudes l and perpendicular amplitude corrections K were calculated [11] in two ways. In the first an assumed force field was employed, using values for the force constants obtained for related molecules, and also using the gas-phase vibrational data for the molecule reported here. In the second the force field data of Durig *et al.* [5] were employed. The two analyses gave very similar values for the vibrational amplitudes and perpendicular amplitude correc-
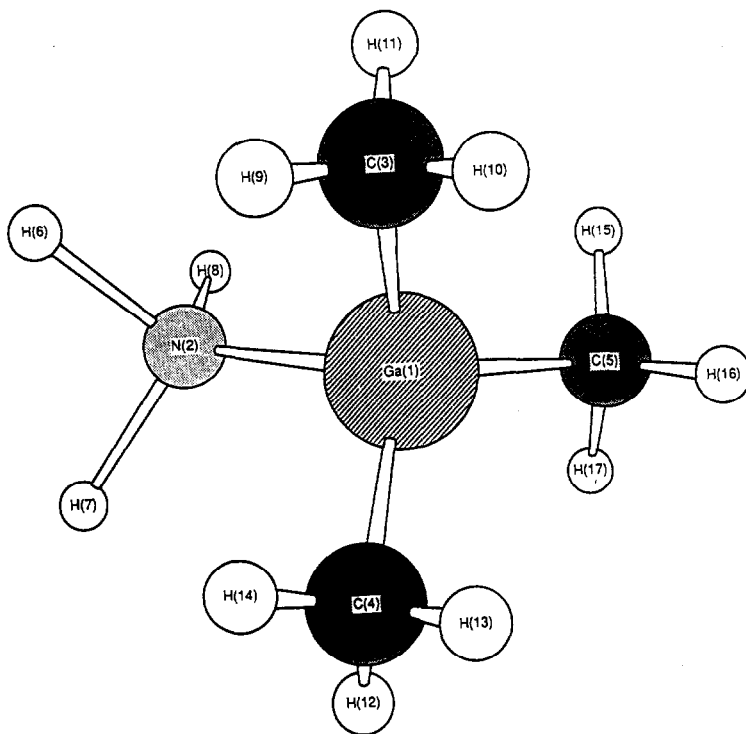

Fig. 2. Diagram of $Me_3Ga \cdot NH_3$ with atom numbering.

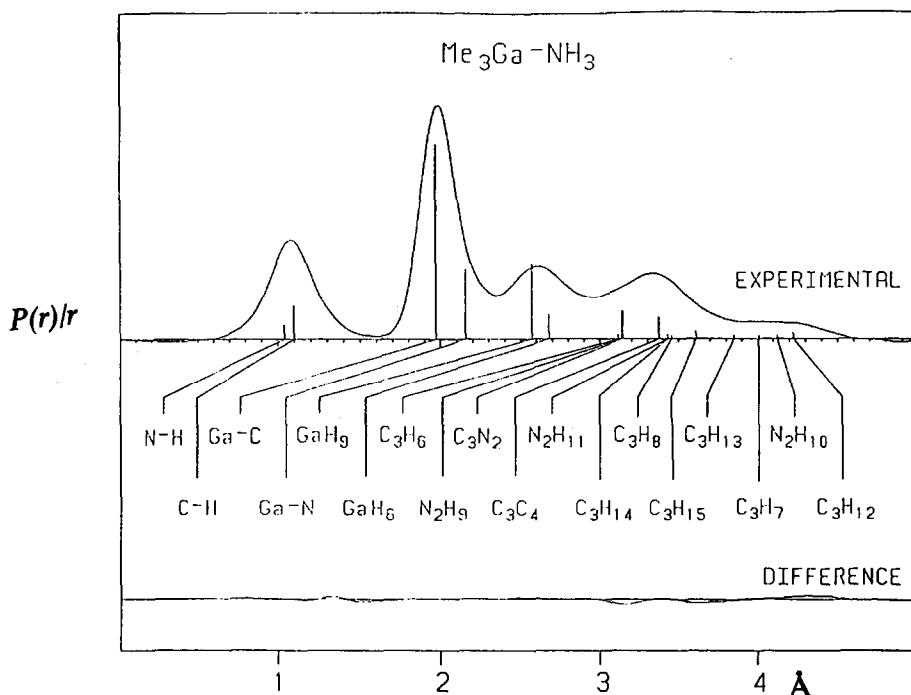Fig. 3. Experimental, theoretical and difference radial distribution curves for $Me_3Ga \cdot NH_3$. These curves were obtained by Fourier inversion of the curves shown in Fig. 1 after multiplication by $Z_{Ga}Z_N/f_{Ga}f_N \cdot \exp(-0.0025s^2)$ and using theoretical data for the unobserved area $s < 2.25$ Å^{-1}. The vertical lines indicate the interatomic distances; their lengths are proportional to the weights of the distances.

tions. The least-squares refinements produced identical values for the variables irrespective of which set of vibrational amplitudes and perpendicular amplitude corrections were used.

Refinements of the structure were carried out by the least-squares procedure [9] based on the intensity curves by adjusting the theoretical curve to the two averaged experimental intensity curves using a unit weight matrix. Six independent parameters were refined simultaneously: the bond distances $r(Ga-N)$, $r(Ga-C)$ and $r(C-H)$, the valence angles N–Ga–C and Ga–C–H and the torsion angle ϕ_1. It was necessary to fix $r(N-H)$, since upon refinement an unreasonable value was produced and the refinement did not converge. This was not surprising as the three $r(N-H)$ distances were under the same peak of the radial distribution curve (Fig. 3) as the nine $r(C-H)$ distances and the two parameters were found to be highly correlated. For similar reasons it was necessary to fix the valence angle Ga–N–H at 109.0°. Refinement of the torsion angle ϕ_2 led to values that carried very large uncertainties and so ϕ_2 was fixed at 60°.

Eight vibrational amplitudes were refined. These were the vibrational amplitudes of all of the bonded distances and those of the non-bonded distances which were thought to be the most influential, namely $r(Ga \cdots H(9))$, $r(Ga \cdots H(6))$, $r(C \cdots N)$, and $r(C \cdots C)$. Some of the amplitudes were tied together (Table 1). The rest of the amplitudes were held constant at the calculated values.

The final bond distances, angles and amplitudes together with the related correlation matrix for the final refinement are given in Table 1 and Table 2 respectively. From the correlation matrix it can be noted that ϕ_1 and the angle N–Ga–C are highly correlated and so it is not surprising that the refined values for ϕ_1 and the angle N–Ga–C, which are 37.5(224) and 101.8(62)° respectively, both carry large uncertainties.

Results and discussion

The electron diffraction data obtained in this study are consistent with molecules of I having a C_3–Ga–N fragment of C_{3v} symmetry. No evidence was obtained for dissociation of the molecule during the experiment. The bond lengths and angles from the final refinement are recorded in Table 1. The most notable values in Table 1 are the values obtained for N–Ga–C (101.8(62)°) and the dependent angle C–Ga–C (115.9(42)°). One might expect, from the predictions of VSEPR theory, that the two angles subtended at the gallium centre would be close to the tetrahedral angle. The value obtained for C–Ga–C is, within experimental error, the same as that found in Me_3Ga (118.6(4)°) [12]. The literature contains reports of the results of electron diffraction studies of the structures of a number of gallium, aluminium and boron compounds having the stoichiometry $X_3M \cdot YR_3$ (where M = B, Al or Ga; X = H, Cl, Br or I, Y = N or P, and R = H or Me) [6,13–21], and the values obtained for the angle X–M–Y are given in Table 3. It is clear that on

Table 1

Final structural parameters for $Me_3Ga \cdot NH_3$ [a]

Parameter	r_g	$l_{refined}$	l_{calc} [b]
r(Ga–N)	2.161(22)	0.108(13)	0.072
r(Ga–C)	1.979(3)	0.055(4)	0.054
r(N–H)	1.045 [c]	0.077(6) [d]	0.075
r(C–H)	1.109(7)	0.082(8) [d]	0.079
∠Ga–N–H	109.0 [c]		
∠N–Ga–C	101.8(62)		
∠Ga–C–H	111.3(16)		
ϕ_1 [e]	37.5(224)		
ϕ_2 [e]	60.0 [c]		
Selected dependent parameters			
r(C $\cdots$ C)	3.348(78)	0.215(34) [f]	0.122
r(Ga $\cdots$ H(6))	2.678(21)	0.144(16) [g]	0.148
r(C $\cdots$ N)	3.211(133)	0.225(12) [f]	0.123
r(Ga $\cdots$ H(9))	2.584(21)	0.144(16) [g]	0.148
∠C–Ga–C	115.9(42)		
R = 0.077 [h]			

[a] Distances (r_g) and amplitudes (l) are in Ångströms and angles (∠) in degrees. Uncertainties, in parentheses, are 2σ plus estimates for the uncertainties in the electron wavelength *etc.* and correlation of the data. [b] Based upon the data of Durig *et al.* [5]. [c] Assumed value. [d] Amplitudes tied together. [e] ϕ_1 describes the position of the H–C bonds with respect to the Ga–N *i.e.* $\phi_1 = \tau_1$(HCGaN) (rotation about Ga–C) and ϕ_2 relates the position of the N–H bonds to the Ga–C bonds *i.e.* $\phi_2 = \tau_2$(HNGaC) (rotation about Ga–N). [f] Amplitudes tied together. [g] Amplitudes tied together. [h] $R = [\Sigma w_i \Delta_i^2 / \Sigma w_i (s_i l_i (\mathrm{obsd}))^2]^{1/2}$, where $\Delta_i = s_i l_i (\mathrm{obsd}) - s_i l_i (\mathrm{calcd})$.

Table 2

Correlation matrix [$\times 100$] for Me$_3$Ga$\cdot$NH$_3$

Parameter	σ[a]	r_1	r_2	r_3	$\angle_1$	$\angle_2$	ϕ_1	l_1	l_2	l_3	l_4	l_5
r(Ga–N)	0.78	100	61	5	−50	−28	24	40	15	41	−68	−3
r(Ga–C)	0.09		100	3	−34	−15	17	25	54	41	−41	−9
r(C–H)	0.25			100	0	−20	−2	−27	2	−1	−3	0
$\angle$N–Ga–C	219				100	25	−88	−19	−10	−22	57	33
$\angle$Ga–C–H	57.8					100	−14	−12	30	−10	38	−37
ϕ_1	791						100	8	6	9	−37	−33
l(N–H)	0.20							100	6	34	−22	5
l(Ga–N)	0.42								100	48	−5	−19
l(Ga–C)	0.12									100	−21	3
l(Ga$\cdots$H)	81.0										100	−2
l(C$\cdots$N)	0.52											100

[a] Standard deviations ($\times 100$) from least squares refinements. Distances and amplitudes are in Ångströms, angles ($\angle$) in degrees.

Table 3

Comparison of values of the angle XMY in adducts $X_3M \cdot YR_3$ (as determined by electron diffraction)

Compound	angle (deg.)	Ref.
$Me_3Ga \cdot NMe_3$	99.3(22)	6
$Br_3Ga \cdot NH_3$	101.5	13
$Cl_3Ga \cdot NH_3$	101.1	14
$Cl_3Al \cdot NMe_3$	104.9(7)	15
$Cl_3Al \cdot NH_3$	101.2	16
$Me_3Al \cdot NMe_3$	102.3(3)	17
$Me_3Al \cdot PMe_3$	100.0(13)	18
$H_3B \cdot NMe_3$	112.2(4)	19
$Cl_3B \cdot NMe_3$	110.8(3)	20
$I_3B \cdot NMe_3$	108.9(4)	21

descending the group from boron to gallium the angle X–M–Y decreases and the X_3M group becomes close to planar. The reasons for this change may be ascribable to the influence of steric interactions in the boron compounds, arising from the relatively short B–N distances, or to the increase in s–p separation as the group is descended, which causes a change from sp^3 (seen with boron) to sp^2 (seen with aluminium and gallium) hybridisation on descending the group. Therefore it appears that in I the gallium atom remains essentially sp^2 hybridised, with the nitrogen atom donating a lone pair of electrons into the p_z orbital of the gallium atom which is perpendicular to the approximately planar Ga–C_3 fragment.

The infrared spectra were recorded of solid films formed by freezing the vapour above a sample of I onto a CsI window at 77 K, and of the gaseous adduct. These spectra show that the adduct is transported intact in the gas phase. No other species are observed and the spectra are in good agreement with those of the solid adduct previously reported [5]. The infrared spectrum of the frozen sample is illustrated in Fig. 4, while the wave numbers of the infrared absorptions are listed in Table 4, where approximate assignments of the bands are also given. One point of interest to emerge from these infrared spectra is the relative weakness in intensity of $\nu_{sym}(Ga-C_3)$, supporting the observation of a near-planar Ga–C_3 unit.
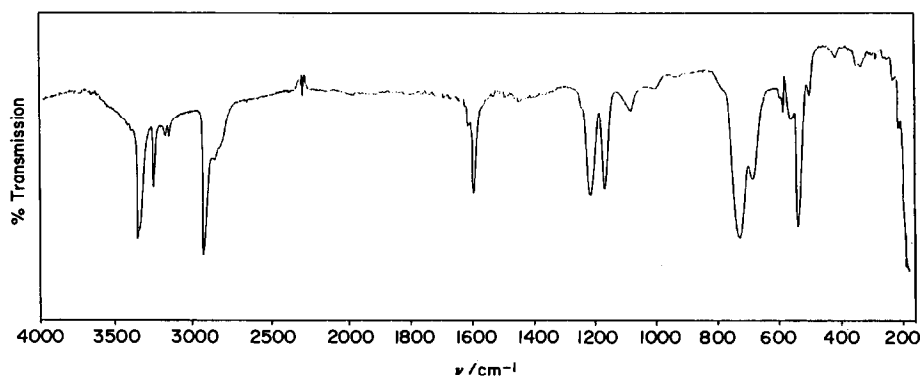

Fig. 4. Infrared spectrum of $Me_3Ga \cdot NH_3$ obtained at 77 K.

Table 4

Observed infrared frequencies for $Me_3Ga \cdot NH_3$

Gas phase ν/cm^{-1}	Solid phase ν/cm^{-1}	Data from ref. 5 ν/cm^{-1} (77 K)	Selected assignments ([5])
	3371(s)	3350(s)	ν_{asym}(N–H)
	3277(m)	3277(m)	ν_{sym}(N–H)
		3267	
	3205(w)	3219(w)	
2958(m)	3183(w)	3187(w)	
2948(s)	2937(s)	2940(s)	ν_{asym}(C–H)
2938(m)	2890(wm)	2882(m)	ν_{sym}(C–H)
	2850(sh)	2832(sh)	
		2331(w)	
		2216(vw)	
		1928(vw)	
		1827(w)	
1591(w)	1607(m)	1610(m)	δ_{as}(NH$_3$)
		1404(vw)	δMe$_3$
	1228(s)	1224(s)	δ_s(NH$_3$)
1204(m)		1207(s)	
1136(vs)	1180(s)	1177(vs)	δ_s(Me)
740(m,br)	735(vs,br)	750(vs)	ρ(Me)
		723(s)	ρ(Me)
	696(ms)	709(s)	ρ(Me)
673(w)		690(sh)	δ(GaCH)
	600(wm)	604(m)	ρ(NH$_3$)
		581(m)	
560(vs)	545(vs)	542(vs)	ν_{asym}(Ga–C)
	516(w)	522(w)	ν_{sym}(Ga–C)
		515(w)	
	350(w)	368(m)	ν(Ga–N)
		357(m)	

A pseudo-tetrahedral N–Ga–C$_3$ unit has C_{3v} symmetry and thus both the $a_1(\nu_{sym}$(Ga–C$_3$)) and $e(\nu_{asym}$(Ga–C$_3$)) modes are infrared active. For a C$_3$–Ga–N moiety that has a planar C$_3$Ga fragment, the local symmetry about the gallium atom remains C_{3v} and so both the a_1 and e modes are still infrared active. The two models may be distinguished, however, by the relative intensities of the infrared bands arising from ν_{sym}(Ga–C$_3$) and ν_{asym}(Ga–C$_3$). For the near planar GaC$_3$ moiety, ν_{sym}(Ga–C$_3$) is predicted to be very weak. This prediction is found to fit the observed spectra reported here. The bands corresponding to ν_{asym}(Ga–C$_3$) and ν_{sym}(Ga–C$_3$) at 545 cm^{-1} and 516 cm^{-1} were found to be strong and weak, respectively, in intensity. In the condensed phase spectrum reported here the ratio of the intensity of ν_{sym} to ν_{asym} is 0.27:1, while in the spectrum of gaseous Me$_3$Ga $\cdot$ NH$_3$, ν_{sym} was too weak to be observed under the conditions used. In their normal co-ordinate analysis of I Durig et al. [5] assign 86% of the intensity of the features they observe at 542 cm^{-1} (observed at 545 cm^{-1} in the present study) to ν_{asym}(Ga–C$_3$) and 94% of the intensity of the band at 522 cm^{-1} (observed at 516 cm^{-1} in the present study) to ν_{sym}(Ga–C$_3$) (our normal co-ordinate analysis gave 92 and 93% respectively). Thus, to a first approximation, for the solid phase

spectrum reported here we can discount any effect of coupling on the intensity ratio of the features seen at 545 and 516 cm^{-1} which are assigned to ν_{asym} and ν_{sym}(Ga–C$_3$) respectively. The low value of the intensity ratio which we observe does reflect the structure of the GaC$_3$ moiety assigned to I.

The Ga–C distance [r_g(Ga–C) = 1.979(3) Å] in Me$_3$Ga · NH$_3$ is slightly longer than that seen in the parent alkyl Me$_3$Ga (1.967(2) Å) [12]; such a lenghtening is expected upon formation of a co-ordination compound. The Ga–N distance (r_g(Ga–N) = 2.161(22) Å) [22] is in accord with that seen in Me$_3$Ga · NMe$_3$ (2.20(3) Å) [6] and H$_3$Ga · NMe$_3$ (2.124(7) Å) and is significantly longer than that in Cl$_3$Ga · NH$_3$ (2.057(11) Å) [14]. The shorter Ga–N distance in Cl$_3$Ga · NH$_3$ is attributable to the influence of the high electronegativity of chlorine. The length of the Ga–N bond in I *suggests* that the bond may be fairly weak, and this suggestion is supported by numerous pieces of evidence. First, the results of our mass spectral analysis of the adduct provide no evidence for a species containing a Ga–N bond. Secondly, ν(Ga–N) occurs at a relatively low wavenumber (350 cm^{-1}) in the infrared spectrum of I. Thirdly, the refinement of the electron diffraction data for I, was found to produce a large vibrational amplitude for the Ga–N bond of 0.108(13) Å (see Table 1) while for H$_3$Ga · NMe$_3$ the corresponding value was 0.061(11) Å [22], in Me$_3$Ga · NMe$_3$ it was 0.058(42) Å [6] and in Cl$_3$Ga · NH$_3$ it was 0.037(13) Å [14]. Finally, it has been reported [5] that it was not possible to obtain a microwave spectrum of I due to its decomposition in which ammonia was produced.

Conclusions

It has been shown that Me$_3$Ga · NH$_3$ (I), the species most likely to be formed when NH$_3$ and Me$_3$Ga (the commonly used precursors for formation of GaN by MOCVD) mixed at room temperature, is transported in the gas phase at room temperature. However, the Ga–N bond appears to be weak and thus it is not surprising that if GaN is to be obtained from the reaction of Me$_3$Ga and NH$_3$ using MOCVD it is essential to have an excess of ammonia because as I is transported into the heated zone of a MOCVD reactor decomposition will take place.

Acknowledgments

References

1 M.A. Khan, D.T. Olson, J.M. van Hove and J.N. Kuznia, Appl. Phys. Lett., 58 (1991) 327.
2 M. Hashimoto, H. Amano, N. Sawaki and I. Akasaki, J. Cryst. Growth, 68 (1984) 163.
3 G.E. Coates, J. Chem. Soc., (1951) 2003.

4 C.A. Kraus and F.E. Toonder, Proc. Nat. Acad. Sci., 19 (1933) 292.

5 J.R. Durig, C.B. Bradley and J.D. Odom, Inorg. Chem., 21 (1982) 1466.

6 V.S. Mastryukov, V.P. Novikov, L.V. Vilkov, A.V. Golubinskii, L.M. Golubinskaya and V.I. Bregadze, Zh. Strukt. Khim., 28 (1987) 122 (English translation).

7 W. Zeil, J. Hasse and L. Wegmann, Z. Instrumentenkd., 74 (1966) 84.

8 K. Tamagawa, T. Iijima and M. Kimura, J. Mol. Struct., 30 (1976) 243.

9 K. Hagen, R.J. Hobson, C.J. Holwill and D.A. Rice, Inorg. Chem., 25 (1986) 3659.

10 L. Schäfer, A.C. Yates and R.A. Bonham, J. Chem. Phys., 56 (1971) 3056.

11 R.L. Hildebrandt and J.D. Weiser, J. Chem. Phys., 55 (1971) 4648.

12 B. Beagley, D.G. Schmidling and I.A. Steer, J. Mol. Struct., 21 (1974) 437.

13 M. Hargittai, I. Hargittai, V.P. Spiridinov and A.A. Ivanov, J. Mol. Struct., 39 (1977) 225.

14 M. Hargittai, I. Hargittai and V.P. Spiridinov, J. Mol. Struct., 30 (1976) 31.

15 A. Almenningen, A. Haaland, T. Hangen and D.P. Novak, Acta Chem. Scand., 27 (1973) 1821.

16 M. Hargittai, I. Hargittai and V.P. Spiridnov, J. Chem. Soc., Chem. Commun., (1973) 750.

17 G.A. Anderson, F.R. Forgaard and A. Haaland, Acta Chem. Scand., 26 (1972) 1947.

18 A. Almenningen, L. Fernholt, A. Haaland and J. Weidlein, J. Organomet. Chem., 145 (1978) 109.

19 K. Iijima, N. Adachi and S. Shibata, Bull. Chem. Soc. Jpn., 57 (1984) 3269.

20 M. Hargittai and I.M. Hargittai, J. Mol. Struct., 39 (1977) 79.

21 K. Iijima and S. Shibata, Bull. Chem. Soc. Jpn., 55 (1982) 2551.

22 P.L. Baxter, A.J. Downs and D.W.H. Rankin, J. Chem. Soc., Dalton Trans., (1984) 1755.